MEMOIRS OF THE SCHOOL OF ENGINEERING, OKAYAMA UNIVERSITY, Vol. 3, No. 1, SEPTEMBER 1968

Mechanism of Fatigue Fracture
(On the Distribution of Plastic Strain around Fatigue Cracks)

Kazuo HONDA and Tetsuro KONAGA

Department of Mechanical Engineering

(Received March 15, 1968)

Broadly speaking, there are three kinds of approaches to investigate the deformation and fracture of materials, that is, the microscopic (metallurgical), macroscopic (mechanical) and theoretical (mathematical) researches. It is necessary, however, to bridge the gap which persists among of them.

Many investigations on the form of plastically deformed zone at a crack tip, the distribution of plastic strain in plastic zone and fracture criterion have been made for the purpose to clarify the mechanism on initiation and propagation of cracks.

In this paper, the authors report the studies, from the standpoint of microscopic views, on the crystal deformation at the tip of cracks in notched specimen during fatigue process.

§ 1. Introduction

Although fracture mechanism, broadly speaking, represents knowledge of the influence of loading and geometry on fracture, in the end, they are usualy associated with the intiation and expansion process of the crack. Many previous workers in relation with those problems have investigated on the strain distributions at the stress concentrated regions, notch root, tip of the crack, from all angles. They are divided into three groups. The first is the "microscopic research" which is due to observations on the distribution of the dislocation by electron microscope and back-reflection microbeam X-Ray diffraction techniques, and the second is "macroscopic research" which deals with the relation between velocity of the crack propagation and applied stress levels, The third is based on "theoretical research" which deals with the analysis of the expansion of the elastic stress distribution around the tip of the crack.

In the present paper, first, the authors introduce three kinds of the mentioned above investigations, and second, the study on the crystal deformation at the tip of the crack in the notched fatigue specimens from the standpoint of microscopic views which has been made by the authors.

§ 2. Previous Investigations

§§ 2.1. Microscopic Research

Some studies on the crystal deformation at the tip of crack or notch root have been made with notched fatigue specimens by Grosskreutz[1),2)], Wood[3)], Taira *et al*[4)]., Karashima *et al*[5),6)]. and Honda *et al*[7)]. from the point of microscopic views which were grounded on the scales of (A), (B) and (C) shown in Fig. 1. These investivations reported that the dislocation arrangement (substracture) introduced at the tip of the crack by fatigue are correlative to the mechanism of its fracture. For example, Grosskreutz pointed out in his papers that in high stacking fault energy materials like aluminum, subgrain formation will always exist at the tip of a crack. Crack propagation occurs along the subgrain boundary because the boundary represents a major source of dislocations which can contribute to the fracture mechanism and because the higher energy of this region will lower the total work necessary to fracture. The others obtained also similar results on the observations by using electron microscope and back-reflection microbeam X-Ray diffraction techniques.

In lower stacking fault energy materials, however, it is probable that the substructure does not form even at the tip of the crack, it

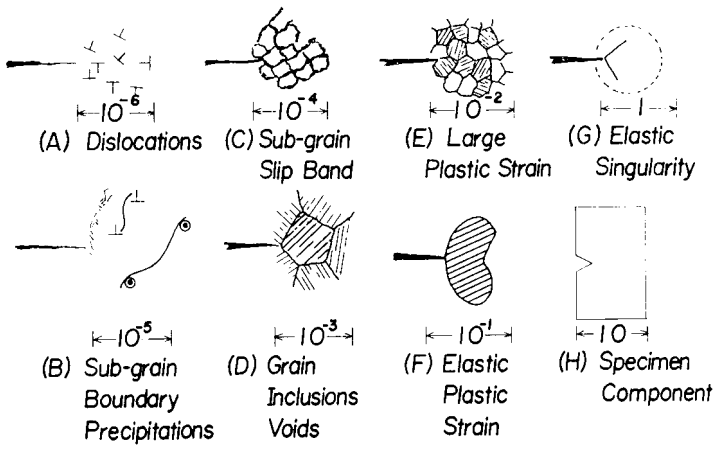

Fig. 1. Schematic illustrations of fracture viewed at different scales.

is considered that the fracture mechanism must be different.

§§ 2.2. Macroscopic Research

The investigations belong to this series are grounded on the scales of (D), (E) and (F) shown in Fig. 1. Some of them deal with crack propagation law. The crack propagation laws have been presented in the past years. They are specifically the work of Head[8], Frost *et al*[9]., McEvily *et al*[10]., Liu[11),12)] and Paris *et al*[13),14)]. In general they treat cracks in infinite sheets subjected to a uniform stress perpendicular to the crack and they relate the crack length, $2a$, to the number of cycles of load applied, N, with the stress range, σ, and material constants C_i. The single form in which all crack propagation laws may be written is

$$\frac{da}{dN} = f(\sigma,\ a,\ C_i) \quad \cdots\cdots(1)$$

Chronologically the first crack propagation law which drew wide attension was that of Head. He employed a mechanical model which consider rigid-plastic work-hardening ahead of a crack tip and elements over the remainder of the infinite sheet. The model required calculations and deductions to obtain a law which may be written as

$$\frac{da}{dN} = \frac{C_1\sigma^3 a^{3/2}}{(C_2-\sigma)\omega_0^{1/2}} \text{ (Head's law)} \cdots\cdots(2)$$

where C_1 depends upon the strain-hardening modulus, the modulus of elasticity, the yield stress and the fracture stress of the material, and C_2 is the yield strengh of the material, Head difined ω_0 as the size of the plastic zone near the crack tip and presumed it was constant during crack propagation. However, Frost *et al.* discovered that the plastic zone size increased in direct proportion to the crack length in his tests.

Frost and Dugdale presented a new approach to crack propagation law. They observed that Head's law shoud be corrected for the variation of the plastic zone size with crack length. They deduced that the corrected result, equation (3), dependents linearly on the crack length, a.

$$\frac{da}{dN} = \frac{C_3\sigma^2 a}{(C_2-\sigma)} \text{(Head's corrected law)} \cdots(3)$$

However, they also argued by dimensional analysis that the incremental increase in crack length da, for an incremental number of stress cycles dN, should be directly proportional to the crack length a, Hence they concluded that (independent of Head's model)

$$\frac{da}{dN} = Ba \quad \cdots\cdots(4)$$

where B is a function of the applied stresses. Then they observed that in order to fit thier experimental data:

$$B = \frac{\sigma^3}{C_4} \quad \cdots\cdots(5)$$

Combining equations (4) and (5) they obtained the law:

$$\frac{da}{dN} = \frac{\sigma^3 a}{C_4} \text{(Frost and Dugdale's law)} \cdots(6)$$

About the same time McEvily and Illg modified a method of analysis of static strength of plates with cracks to obtain a theory of crack propagation. Thier arguments were as follows: Presuming that a crack tip in a material has a characteristic (fictitious) radius ρ_1, which allows computation of the stress σ_0, in the element at the crack tip using elastic stress-concentration factor concepts, the stress σ_0 is

$$\sigma_0 = K_N \sigma_{net} \quad \cdots\cdots(7)$$

where K_N is the stress-concentration factor

and ρ_{ent} is the net area stress at the cracked section. For the configuration used here, i. e., an infinite plate with uniform stress σ

$$K_N = 1+2\left(\frac{a}{\rho_1}\right)^{\frac{1}{2}} \quad \cdots\cdots(8)$$

which is based on the elastic solution for an elliptical hole of semimajor axis a and end radius ρ_1.

$$\sigma_{net} = \sigma \quad \cdots\cdots(9)$$

and substituting equations (8) and (9) into (7) gives

$$\rho_0 = \sigma\left[1+2\left(\frac{a}{\rho_1}\right)^{\frac{1}{2}}\right] \cdots\cdots(10)$$

Based on considerations that under cyclic loading work-hardening at the crack tip will raise the local stress to a fracture stress, they concluded that the crack-extension rate will be a function of σ_0 or

$$\frac{da}{dN} = F\{\sigma_0\} = F\{K_N\sigma_{net}\}$$
(McEvily and Illg's law)···(11)

Therefore for the special configuration of interest here, i. e., introducing equations (7), (8) (9) and (11) into (12), we have

$$\frac{da}{dN} = F\left\{\sigma\left[1+2\left(\frac{a}{\rho_1}\right)^{\frac{1}{2}}\right]\right\} \quad \cdots\cdots(12)$$

which is the desired form in this disccusion upon considering ρ_1 to be a material constant, in likeness to the C_i.

McEvily and Illg go on in an empirical manner to obtain the form of the function $F\{\ \}$, and suggest

$$\log_{10}\left(\frac{da}{dN}\right) = 0.00509K_N\sigma_{net} - 5.472 - \frac{34}{K_N\sigma_{net}-34}$$
(McEvily and Illg's law empillically extended) ·····(13)

It should be noted by the reader that McEvily and Illg's law, equations (11) and (13), are not restricted to the special configuration here, as well the case for the laws of Head, and Frost and Dugdale. The applicability to other configurations and an additional similarity to Paris' work will warrant later comments.

Independent of McEvily and Illg, Paris propose a crack propagation theory at the same time. It is based on the following arguments: Irwin's stress-intensity factor k reflects the effect of external load and configration on the intensity of the whole stress field around a crack tip. Moreover, for various configurations the crack tip stress fiele always has the same form (i. e., distribution). Therefore it was reasoned that the intensity of the crack tip stress field as represented by k should control the rate of crack extention. That is so say:

$$\frac{da}{dN} = G\{k\} \quad \cdots\cdots(14)$$

In treating the special configuration of interest in this disccusion, it should first be observed that (10)

$$k = \sigma a^{\frac{1}{2}} \quad \cdots\cdots(15)$$

whereupon equation (14) may be specialized to read:

$$\frac{da}{dN} = G\{\sigma a^{\frac{1}{2}}\} \cdots\cdots(16)$$

Somewhat later, Liu restated Frost and Dugdale's dimensional analysis in a much more elegant form and argued that the crack growth rate should depend linearly on the crack length; i. e.,

$$\frac{da}{dN} = Ba \quad \text{(Liu's law)} \cdots\cdots(17)$$

which is the same result as equation (4). Liu then presumed that B was in general a function of stress range (and meam stress); i. e.,

$$B = B(\sigma) \quad \cdots\cdots(18)$$

In a subsequent work, Liu notes that mean stress is of secondery influence and, using a model of crack extension employing an idealized elastic-plastic stress-strain diagram and a concept of total hysteresis energy absorption to failure, reasons that

$$B(\sigma) = C_5\sigma^2 \quad \cdots\cdots(19)$$

which combined with equation (17) gives

$$\frac{da}{dN} = C_5\sigma^2 a \text{ (Liu's modified law)} \cdots(20)$$

On the other hand, there are many investigations which dealed with the observations on the plastic zones, i. e., initial fatigue cracks[15], spread of fatigue cracks[16], slipband damage and extrusion and intrusion[17], using a microscope. Here, the authors shall give up them to intoduce.

§§ 2.3. Theoretical Research

A general survey of the results of elastic

stress analyses of cracked bodies is the basic objective of these theoretical researches.

In his famous paper, Griffith[18] made use of the stress solution provided by Inglis for a flat plate under uniform tension with an elliptical hole which could be degenerated into a crack. However, neither Griffith nor his predecessors had the knowledge of stress fields near cracks which is now available, so as a consequence, he devised an energyrate analysis of equilibrium of cracks in brittle materials. Sneddon[19] was the first to give stress field expansions for crack tips for two individual examples; however it was only later that Irwin[20] and Williams[21] recognized the general applicability of these field equations and extended them to the most general case for an isotropic elastic body.

The surface of a crack, since they are stress-free boundaries of the body near the crack tip, are the dominating influence on the distributions of stresses in that vicinity. Other remote boundaries and loading forces affect only the intensity of the load stress field.

The stress fields near crack tips can be divided into three basic types, each associated with a local mode of deformation as illustrated in Fig. 2. The opening mode, I, is associated

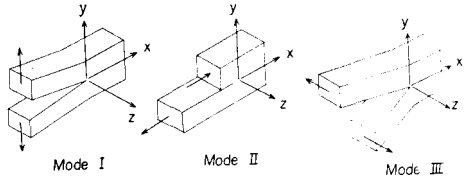

Fig. 2. Modes of deformation of a crack.

with local displacement in which the crack surfaces move directly apart (symmetric with respect to the x-y and x-z planes). The edge-sliding mode, II, is characterized by displacements in which the crack surfaces slide over one another perpendicular to the leading edge of the crack (symmetric with respect to the x-y plane and skew-symmetric with respect to the x-z plane). Mide III, tearing, finds the crack surfaces sliding with respect to one another parallel to the leading edge (skew-symmetric with respect to the x-y and x-z planes). The superposition of these three mode is sufficient to describe the most general case of crack tip deformation and stress fields.

The most direct approach to determination of the stress and displacement fields associated with each mode follows in the manner of Irwin, based on the method of Westergaard. Modes I and II can be analyzed as plane-extensional problems of the theory of elastisity which are subdivided as symmetric and skew-symmetric, respectively, with respect to the crack plane. Mode III can be regard as the pure shear (or torsion) problem. Referring to Fig. 3 for notation, the resultand stress and displacement fields are given (detail calculation process are neglected).

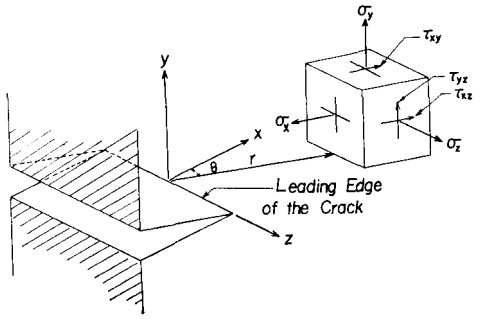

Fig. 3. Coordinates measured from the leading edge of a crack and the stress components in the crack tip stress field.

Mode I

$$\left.\begin{aligned}
\sigma_x &= \frac{K_I}{(2\pi r)^{1/2}}\cos\frac{\theta}{2}\left[1-\sin\frac{\theta}{2}\sin\frac{3\vartheta}{2}\right]\\
\sigma_y &= \frac{K_I}{(2\pi r)^{1/2}}\cos\frac{\theta}{2}\left[1+\sin\frac{\theta}{2}\sin\frac{3\vartheta}{2}\right]\\
\tau_{xy} &= \frac{K_I}{(2\pi r)^{1/2}}\sin\frac{\theta}{2}\cos\frac{\theta}{2}\cos\frac{3\vartheta}{2}\\
\sigma_z &= \nu(\sigma_x+\sigma_y),\quad \tau_{xz}=\tau_{yz}=0\\
u &= \frac{K_I}{G}\left[\frac{r}{2\pi}\right]^{\frac{1}{2}}\cos\frac{\theta}{2}\left[1-2\nu+\sin^2\frac{\theta}{2}\right]\\
v &= \frac{K_I}{G}\left[\frac{r}{2\pi}\right]^{\frac{1}{2}}\sin\frac{\theta}{2}\left[2-2\nu-\cos^2\frac{\theta}{2}\right]\\
w &= 0
\end{aligned}\right\}\cdots(21)$$

Mode II

$$\left.\begin{aligned}
\sigma_x &= -\frac{K_{II}}{(2\pi r)^{1/2}}\sin\frac{\theta}{2}\left[2+\cos\frac{\theta}{2}\cos\frac{3\vartheta}{2}\right]\\
\sigma_y &= \frac{K_{II}}{(2\pi r)^{1/2}}\sin\frac{\theta}{2}\cos\frac{\theta}{2}\cos\frac{3\vartheta}{2}\\
\tau_{xy} &= \frac{K_{II}}{(2\pi r)^{1/2}}\cos\frac{\theta}{2}\left[1-\sin\frac{\theta}{2}\sin\frac{3\vartheta}{2}\right]\\
\sigma_z &= \nu(\sigma_x+\sigma_y),\quad \tau_{xz}=\tau_{yz}=0\\
u &= \frac{K_{II}}{G}\left(\frac{r}{2\pi}\right)^{\frac{1}{2}}\sin\frac{\theta}{2}\left[2-2\nu+\cos^2\frac{\theta}{2}\right]
\end{aligned}\right\}\cdots(22)$$

$$v = \frac{K_{II}}{G}\left(\frac{r}{2\pi}\right)^{\frac{1}{2}} \cos\frac{\theta}{2}\left[-1+2\sin^2\frac{\theta}{2}\right]$$

$$w = 0$$

Mode III

$$\left.\begin{aligned} \tau_{xz} &= -\frac{K_{III}}{(2\pi r)^{1/2}}\sin\frac{\theta}{2} \\ \tau_{yz} &= \frac{K_{III}}{(2\pi r)^{1/2}}\cos\frac{\theta}{2} \\ \sigma_x &= \sigma_y = \sigma_z = \tau_{yx} = 0 \\ w &= \frac{K_{III}}{G}\left(\frac{2r}{\pi}\right)^{1/2}\sin\frac{\theta}{2} \\ u &= v = 0 \end{aligned}\right\} \quad \cdots\cdots(23)$$

Equations (21) and (22) have been written for the case of plane strain but can be change to plane stress easily by taking $\sigma_z = 0$ and replacing Poisson's ratio, ν, in the displacements with an appropriate value. Equations (21), (22) and (23) have been obtained by neglecting higher-order terms in r. Hence, they can be regarded as a good approximating in the region where r is small compared to other planar (x-y plane) dimensions of a body such as crack length and exact in the limit as r approaches zero.

The parameters, K_I, K_{II} and K_{III} in the equations are stress intensity factors for the corresponding three types of stress and displacement fields. It is important to notice that the stress intensity factors are not dependent on the coordinates, r and θ, hence they control the intensity of the stress fields but not the distribution for each mode. For dimensional considerations of Eqs (21), (22) and (23), it can be observed that the stress intensity factors must contain the magnitude of loading forces linearly for linear elastic bodies and must also depend upon the configuration of the boby including crack size. Consequently, stress intensity factors may be physically interpreted as parameters which reflect the redistribution of stress in a body due to the introduction of a crack, and in particular they indicate the type (mode) and magnitude of force transmission through the crack tip region.

Now, though those stress intensity factors, K_I, K_{II} and K_{III} are changed[22] with the shapes of the crack in the infinite bodies, its calculation methods in each case are neglected, here,

§ 3. Authors Investigation

§§ 3.1. Experimental Methods

(1) Fatigue Specimen and Fatigue Testing Machine

The specimens used in the series of experiments were pure copper (99.999%) and low carbon steel (0.1%C). Shape and dimensions are shown in Fig. 4. Before testing, copper

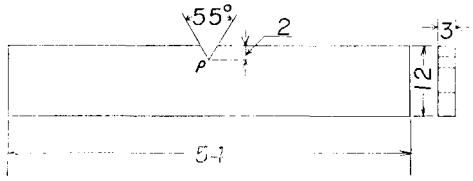

Fig. 4. Fatigue specimen and dimensions.

and low carbon steel specimens were annealed for 2hrs at 400°C and for 2hrs at 750°C under vacuum respectively, furnace cooled and electro-polished. As for electro-polishing solutions, (H_3PO_4-CH_3OH-H_2O) solution was prepared for pure copper specimen, and (H_3PO_4-CrO_3) solution for low carbon steel.

Nishihara's type plane bending fatigue testing machine was used, after it was recomposed to fit the present experiment. The speed of stress repetitions was about 1000 cycles per minute.

(2) Observation by Electron Microscope

For electron microscope, carbon replicas of the fatigued specimen were observed by a two stage faxfilm-carbon process and were shadowed with chromium, the replicas were examined in a JEM-6A electron microscope operating at 50kV.

(3) Back-Reflection Microbeam X-Ray Diffraction Technique

Microbeam X-Ray used in this experiment was collimated by double slits ($100\mu^{\phi}$-$50\mu^{\phi}$) because of the large focal spot on the target of the X-Ray tube. The angle of this microbeam X-Ray was approximately 1.2×10^{-3} radians. Accordingly, resolution power is about 0.4μ if the specimen-film distance is 20 mm. Size of area on the specimen irradiated by X-Ray was about 150μ in diameter.

X-Ray micro-camera is composed of the camera casette, specimen holder and optical microscope. As the specimen holder can be moved up and down and right, and left, and also rotated in horizontal and vertical planes

with high accuracy, it is possible to direct the beam to the desired position on the specimen.

Micro lattice strain and misorientation show that the degree of deformation in crystals are obtained by measuring the widths of radial and tangential directions of the diffraction spots on the film, respectively.

This method has been exploited by Hirsch[23], and applied to various investigations by many workers. In the present study the authors adopted a method which was modified by Taira and Hayashi[4]. According to it, micro lattice strain and misorientation are given by the following formula, respectively.

$$\Delta d/d = \frac{\cos^2 2\theta}{\tan \theta} \cdot \frac{\Delta S_R}{2R_0}$$

and

$$\beta = \frac{\cos 2\theta}{\sin \theta} \cdot \frac{\Delta S_T}{2R_0}$$

where

$\Delta d/d$; micro lattice strain

β ; misorientation

θ ; Bragg's angle

R_0 ; specimen-film distance

ΔS_R, ΔS_T ; ΔS_R-S_{R0}, ΔS_R-S_{T0}

S_R and S_T are widths in the radial and tangential directions of the diffraction spot on the film, S_{R0} and S_{T0} are breadth in radial and tangential directions on it in annealed crystal, respectively.

§§ 3.2. Experimental Results and Discussions

(1) Observation Due to Electron Microscope

Figs. 5 (a), (b) show the features at the tip of non-propagating crack* which was obtained under fatigue process with reversed stress $\sigma_n = 0.69\,kg/mm^2$, cyclic number $N = 1.7 \times 10^7$ and crack length $l_c = 0.03\,mm$.

The optical micrograph (Figs. 5(a)) shown an initiation of the non-propagating crack (N. P. C.) at the first grain boundary in notch root, the propagating along the grain boundary and the termination at the next grain boundary. The detailed feature of the tip of crack is not visible in the micrograph, but visible in electron micrograph, shown in Figs. 5(b). Crack B propagates along slip bands and terminates at the next grain boundary. On the other hand, crack A propagates along grain boundary and stops at a twin boundary.

Figs. 6(a) and (b) show also the feature at the tip of propagating crack (P. C.) under $\sigma_n = 1.15\,kg/mm^2$, $N = 8.6 \times 10^6$ and $l_c = 1.20\,mm$. Fatigue cracks formed in the case of P. C, are

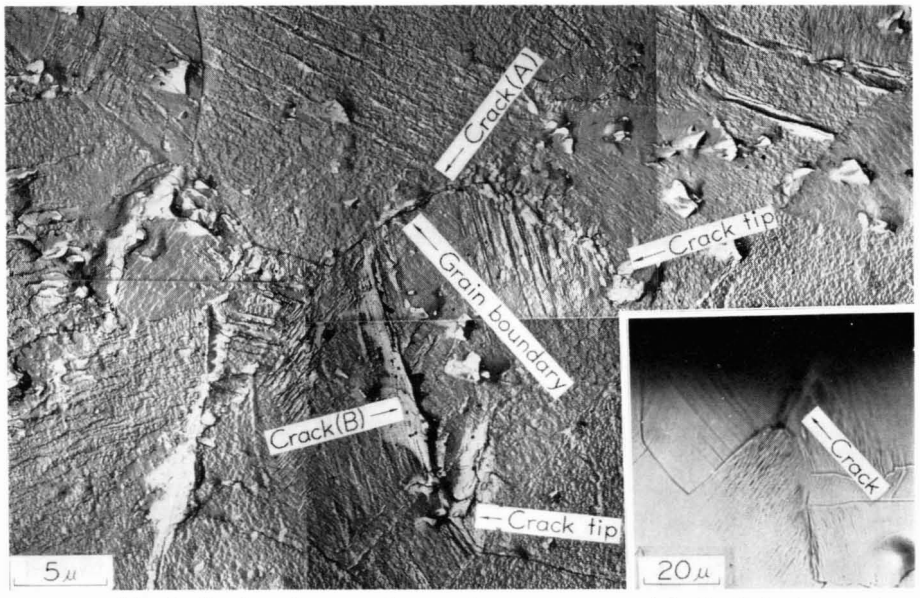

(b) Replication electron micrograph. (a) Optical micrograph.

Fig. 5. Tip of non-propagating crack in pure copper specimen.

* The authors regarded the crack as N. P. C. because a velosity of the crack propagation R_c is 1.7×10^{-9}mm/cycle.

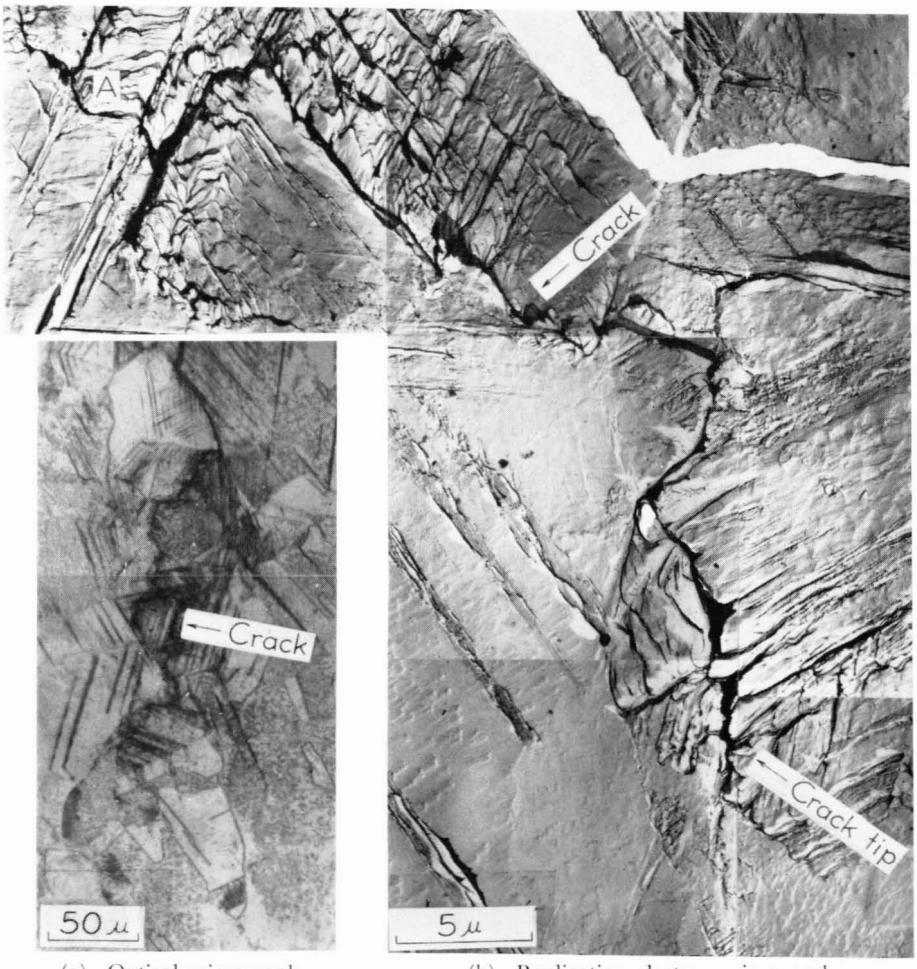

(a) Optical micrograph. (b) Replication electron micrograph.

Fig. 6. Tip of propagating crack in pure copper specimen.

generally along grain boundary as shown in Figs. 6(a). Figs. 6(b) is an electron micrograph showing detailed feature at the tip of P. C., from which it is observed that the crack propagates along grain boundary with occasional propagation along slip bands or cross slip bands (Figg. 6(b) A). It seems that the cross slip band crack results from the influence of the direction of maximum tensile stress.

As mentioned above, it has been reported that a close correlation between the propagation of the crack and the presence of the plastically deformed region (plastic region)** at the tip of the crack can be found. The authors attempted to discuss the experimental results from this respect.

Comparison of Fig. 5(b) and Fig. 6(b) shown that as in the case of P. C., no visible plastic region is present at the tip of N. P. C. It seems that these observations are contrary to the experimental result by Frost *et al.* according to which there is a plastic region at the tip of crack, and the extension is in proportion to the crack length. But the two experimental observations do not contradict each other qualitatively. Namely, the plastic region pointed out by Frost *et al.* is one of the optical microscopic order, in which electron microscope can fied out the cracks.

Fig. 7 shows a feature at the tip of P. C. in an annealed low carbon steel during fatigue process, $\sigma_n = 5.00\,\mathrm{kg/mm^2}$, $N = 5.0 \times 10^5$ and $l_c = 0.98\,\mathrm{mm}$. The crack stops at a grain boun-

** The term of plastically deformed region is used in microstructural observation indicates the region in which slip bands distribute or even if slip bands are not so clear in which heterogeneous deformation occur by slip.

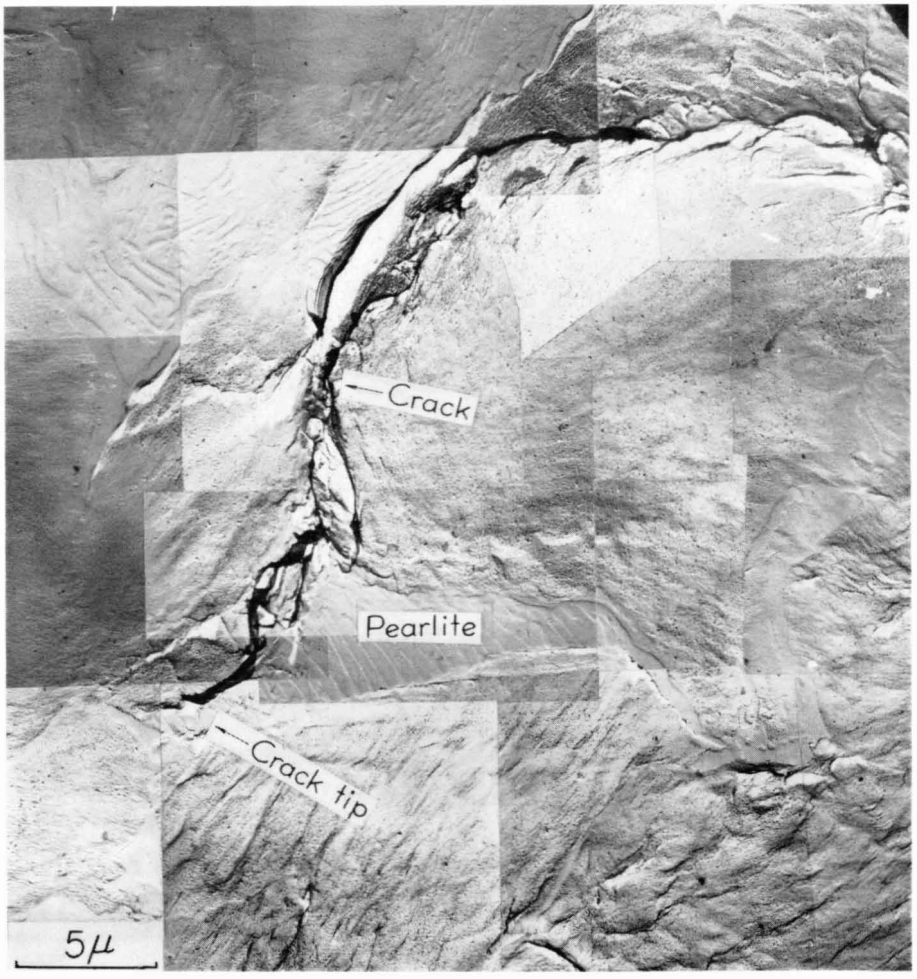

Fig. 7. Tip of propagating crack in low crabon steel.

dary between ferrite and pearlite, and a plastic region (wavy slip bands) is observed ahead of the tip of the crack. The authors have not found yet what factors cause a difference between pure copper and low carbon steel as to the presence of the plastic region at the tip of P. C., and they continue the experiments along this line to make clear the factors.

(2) Observations Due to Microbeam X-Ray Diffraction

In Fig. 8, micro lattice strain $\Delta d/d$ and misorientation β measured from various diffraction spots obtained from deformed crystal at the tip of P. C. using CuKα radiations, are plotted against the distance from the crack tip. It is found that the values of micro lattice strain and misorientation decrease extremly at 0.2 or 0.4mm crack tip, and remain approximately the same feature from there. Fig. 9 of N. P. C. indicates also the same inclination as the case of P. C.

Fig. 10 is prepared to compare the characters in the plastic regions at the tips of P. C. and N. P. C. From these experimental results, it is concluded that there is no difference in the inclination of the changes of micro lattice strain and misorientation, but there are differences in the values themselves at the crack tips. The values at the tip of N. P. C. are equal to those at 0.2 or 0.4mm from the tip of P. C. This is very important because it is considered that the difference of the values determines whether the crack propagates or not.

Figs. 11 and 12 show the relation between the crack length and the modes of the plastic region at the tip of the P. C. in pure copper during fatigue process, with repeated stress

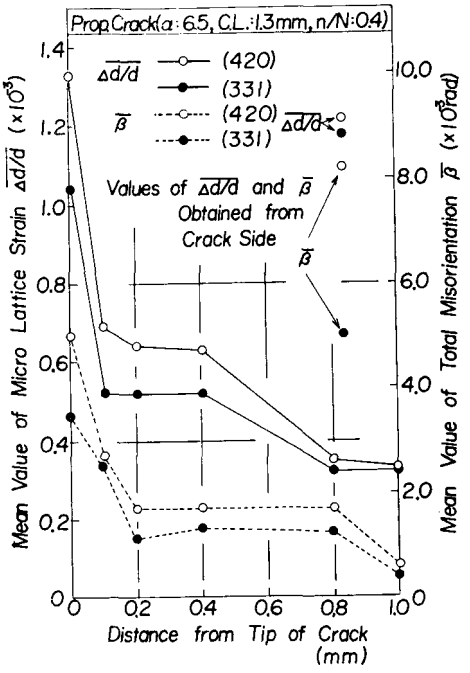

Fig. 8. Distributions of $\overline{\Delta d/d}$ and $\bar{\beta}$ at the tip of propagating crack

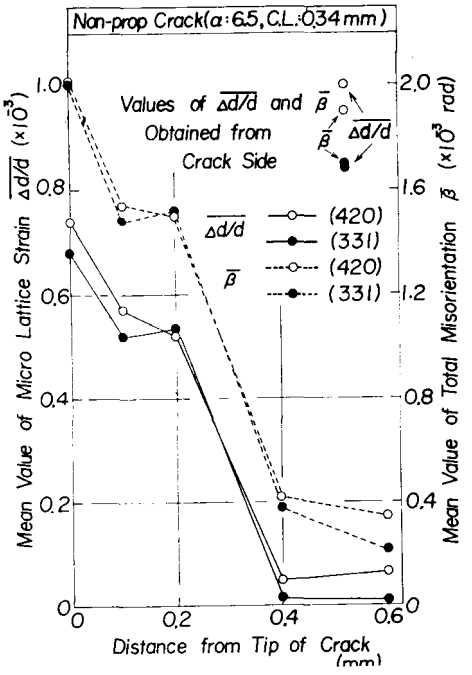

Fig. 9. Distributions of $\overline{\Delta d/d}$ and $\bar{\beta}$ at the tip of non-propagating crack.

$\sigma_n = 2.0\,\mathrm{kg/mm}$ and stress concentration factor $\alpha = 6.5$ and 4.75, respectively. That is, distributions of the plastic region around a tip of a crack are examined in three directions,

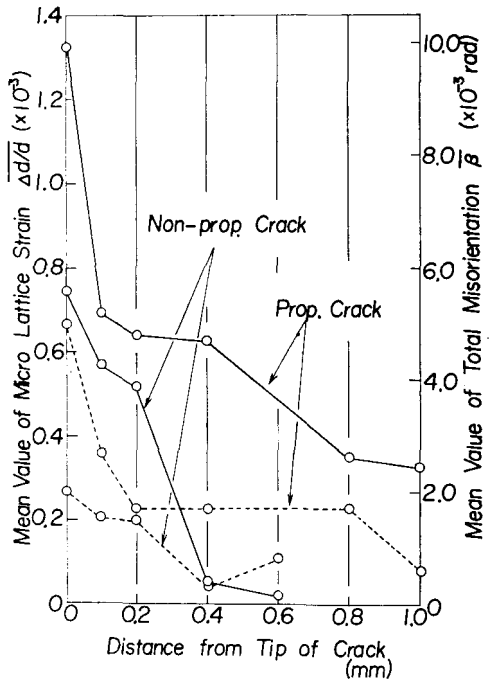

Fig. 10. Comparison of the modes of distributions of $\overline{\Delta d/d}$ and $\bar{\beta}$ at the tip of propagating and non-propagating cracks.

along the crack propagation, normal to one of the crack propagation and 45° to one of the crack propagation, in three stages during fatigue process.

These experimental results give us various informatoins. First, there is no correlation between expansion of plastic region at the crack tip and the crack length. The extension is approximately constant. In particular, this is very clear concerning the changes in the values of misorientation. Second, the values of micro lattice strain and misorientation plotted against the distance from crack tip, change in same way as Figs. 8 and 9. Third, paying attention to the distributions of plastic region in each direction, there is no particular difference between the directions. In other words, the distribution of the values of misorientation obtained from deformed crystal at the tip of a crack is such that the same values in the misorientation exist on concentric circles with center at the tip of the crack. Regarding the micro lattice strain, however, it is not possible to conclude the same.

Recently, the studies by means of X-Ray microbeam technique on the plastic region developed around fatigue crack have been

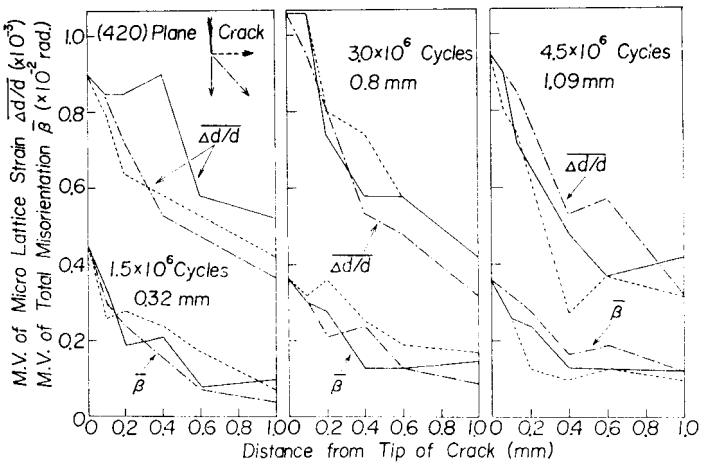

Fig. 11. Correlation between extension of plastic region at the tip of crack and crack length in fatigue process, $\alpha=6.5$, $\sigma_a=2.0\,\mathrm{kg/mm^2}$.

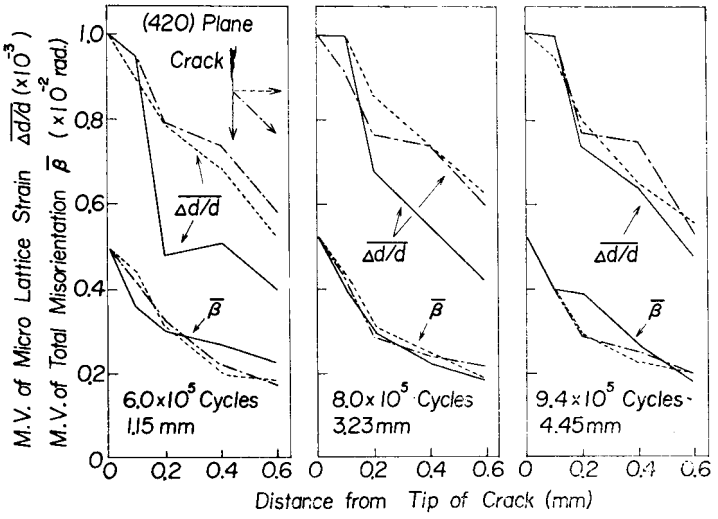

Fig. 12. Correlation between extension of plastic region at the tip of crack and crack length in fatigue process, $\alpha=4.75$, $\sigma_a=2.0\,\mathrm{kg/mm^2}$.

performed by Taira *et al.* (carbon steel) and Karashima *et al.* (pure copper, α-brass and aluminum). Taira *et al.* revealed the relation between the change in micro-stracture at the tip of P. C. and various propagating rate of crack, and discussed the mechanism of crack propagation on the basis of observed results. Karashima *et al.* investigated the formation substracture around fatigue cracks by means of X-Ray microbeam and transmission electron microscope techniques. Comparing with the modes of the plastic region at the tip of P. C. between the experimental results obtained by the authors and Taira *et al.* or Karashima *et al.*, a good correlation can be found.

As mentioned above, to correlative information on the feature at the tip of the crack during fatigue process, the authors carried out parallel examinations by optical, replication electron microscopies and microbeam X-Ray diffraction. A summary of these results is shown in Fig. 13. The optical microscope uncovered the plastic region composed of slip striations at the tip of crack, in which electron microscope showed the crack, and no obvious plastic region was found at the tip of crack. Moreover, the authors revealed a good cor-

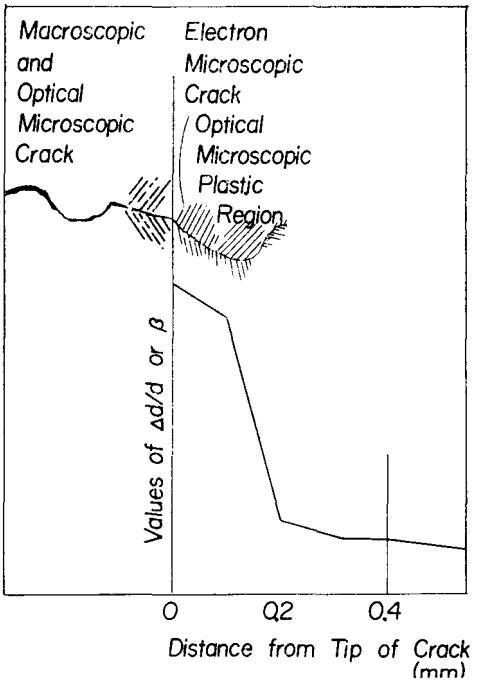

Fig. 13. Schematic illustration of a correlation of the results obtained from optical, replication electron microscope and microbeam X-ray diffraction analysis.

relation between the examination results of microstructural observation and microbeam X-Ray diffraction. That is, the place of about 0.2mm distance far from the crack tip where values of micro lattice strain and misorientation decrease extremly, agreed well with the tip of crack observed by electron microscope.

§ 4. Conclusions

Many interesting features were obtained from the authors experimental results, and the conclusions are as follows;

(1) The crack started in the trace of the slip striations, and eventually spreaded along the persistent slip band. N. P. C. stopped in the first grain or its boundary.

(2) The extension of the plastic region formed around the P. C. tip observed by the electron microscope was greater than that of N. P. C.

(3) Quantitative investigation by means of back-reflection X-Ray microbeam diffraction technique pointed out that the values of the micro lattice strain and misorientation decreased extremly at about 0.2mm from the tip of P. C. These values were equal to those at the tip of N. P. C.

(4) The point 0.2mm from the tip of the P. C. matched well the location of the tip of the P. C. observed by replication electron microscope.

References

1) J. C. Grosskreutz, J. Appl. Phys., **34**, (1963) 372
2) J. C. Grosskreutz, G. G. Shaw, Phil. Mag., **10**, (1964) 961
3) W. A. Wood, Trans. Met. Soc. AIME, **230**, (1964) 511
4) S. Taira and S. Hayashi, JIME, **33**, (1967) 1
5) S. Karashima, H. Oikawa and T. Ogura, JIM, **31**, (1967) 669
6) *ibid* 674
7) T. Konaga and K. Honda, Proc. 11th Jap. Cong. Mat. Res., (1968) 97
8) A. K. Head, Phil. Mag., **44**, (1953) 925
9) N. E. Frost and D. S. Dugdale, J. Mech. Phys. Solids, **6**, (1958) 92
10) A. J. McEvily and W. Illg, NACA Tech. Note **4394** (1958)
11) H. W. Liu, J. Basic Eng. Trans. ASME, **83**, (1961) 23
12) *ibid* **85**, (1963) 116
13) P. C. Paris, M. P. Gomez and W. E. Anderson, Trend Eng., **13**, (1961) 9
14) G. C. Sih, P. C. Paris and F. Erdogan, J. Appl. Mech. Trans. ASME, **28**, (1962) 306
15) G. C. Smith, Proc. Roy. Soc., **A242**, (1957) 189
16) N. E. Erost and C. E. Phillips, Proc. Roy. Soc., **A242**, (1957) 216
17) P. J. E. Forsyth and C. A. Stubbington, J. Inst. Met., **83**, (1954) 395
18) A. A. Griffith, Trans. Roy. Soc., **221**, (1920) 163
19) I. N. Sneddon, Proc. Roy. Soc., **A187**, (1946) 229
20) G. R. Irwin, J. Appl. Mech. Trans. ASME, **24**, (1957) 45
21) M. L. Williams, J. Appl. Mech. Trans, ASME, **24**, (1957) 104
22) H. Neuber, Kerbspannungslehre, Springen, Berlin, (1958)
23) P. B. Hirsch, Acta Cryst., **5**, (1953) 162